IEEE/CSC & ESAS SUPERCONDUCTIVITY NEWS FORUM (global edition), January 2016.
MT-24 preprint 3OrAC_02. Submitted to *IEEE Trans. Appl. Supercond.* for possible publication.

Quench protection of very large, 50 GJ class and high-temperature superconductor based detector magnets

Matthias Mentink, Alexey Dudarev, Tim Mulder, Jeroen Van Nugteren and Herman ten Kate

***Abstract*—An investigation is performed on the quench behavior of a conceptual 50 GJ 8 T high-temperature-superconductor-based solenoid. In this design, a 50 kA Conductor-On-Round-Core Cable-In-Conduit conductor utilizing ReBCO technology is envisioned, operating at 40 K. Various properties such as resistivity, thermal conductivity, and heat capacity are very different at this temperature which affects the quench behavior.**

It is found that the envisioned conductor is very stable with an MQE of about 2 kJ. However the quench propagation velocity is typically about 20 mm/s so that creating a wide-spread normal zone throughout the coil is very challenging. Moreover an extraction voltage exceeding 20 kV would be required to ensure a hot-spot temperature below 100 K once a thermal runaway occurs.

A novel concept dubbed 'Rapid Quench Transformation' (RQT) is proposed whereby the superconducting conductor is co-wound with a normal conductor to achieve a high degree of inductive coupling. This geometry allows for a significant electric noise reduction, thus enabling low-threshold quench detection. The secondary circuit is connected in series with a stack of diodes, not allowing current transfer during regular operation, but very fast current transfer once a quench is detected. With this approach, the hot-spot temperature can be kept within 20 K of the cold mass temperature at all times, the hot-spot temperature is well below 100 K and just under 80% of the stored energy can be extracted during a quench.

***Index Terms*—detector magnet, CORC, cable-in-conduit conductor, quench protection**

I. Introduction

The ATLAS magnet group at CERN is developing ReBCO-based Conductor-On-Round-Core (CORC) Cable-In-Conduit Conductors (CICC) for use in future detector magnets. The CORC concept [1] is well suited for utilization in a cable-in-conduit layout and benefits from the superior superconducting properties of the ReBCO tape in combination with good mechanical properties and excellent stability. With this technology, high-current cable-in-conduit conductors can be fabricated able to operate at elevated temperature and high magnetic field in a high-stress environment thus significantly extending to attainable performance in NbTi-based detector magnets. The ongoing development of this conductor type is discussed elsewhere [2], [3], [4], [5]. The advantage of operating at an elevated temperature is that the cooling cost is significantly reduced. For instance, according to the Carnot's cooling theorem, cooling down to 40 K requires over ten times less power than cooling to 4.5 K. Even more importantly, due to enhanced conductor stability the risk of training and degradation can be largely avoided.

All authors are affiliated with CERN. The primary author (email: matthias.mentink@cern.ch) is with the ATLAS magnet group, Physics Department, CERN, 1217 Meyrin, Switzerland.

While the CORC-CIC conductor concept shows clear promises for the future, a key issue that needs to be addressed is quench protection. Various classical quench protection solutions are challenging to apply to a very large magnet system, and an acceptably low hot-spot temperature during a quench is difficult to achieve.

A very large 50 GJ HTS-based magnet system is presented that operates at 40 K with an 8 T magnetic field in the bore (section III). Thermal simulations are performed to determine the minimum quench energy, and a 'weak-spot' scenario is investigated to determine the behavior during a thermal runaway (section IV). A novel solution is proposed that addresses two quench-related problems simultaneously (Fig. 1). A co-wound geometry comprising a superconducting and a normal conductor is used to significantly reduce the electrical noise on the voltage taps, thus enabling low-threshold quench detection (section V), and the same geometry features a rapid current transfer from the primary to the secondary circuit after quench detection (section VI). In general the RQT concept significantly reduces hot-spot dissipation immediately after quench detection while homogeneously heating up the entire magnet. This concept may be applied in various ways (section VII), in a single magnet or in multiple magnets, and in variations where the energy is either mostly extracted or entirely dissipated in the cold mass. Here the concept is applied to achieve relatively fast quench recovery and to extract most of the stored magnetic energy. The concept does not result in additional heating during ramping and does not require additional external power (beyond the power sources for the control logic and the breaker): It simply involves opening a breaker to induce current discharge.

II. Conductor-On-Round-Core (CORC) Cable-In-Conduit Conductor (CICC) Geometry

A. General description

The CORC strand technology involves wrapping ReBCO tapes on a core [1]. The tapes are wound in multiple layers, where each layer is wound either clock-wise or counter-clockwise to minimize the solenoidal magnetic field component inside the strand. With this technology an engineering current density of 340 A/mm^2 at 4.2 K and 17 T was recently demonstrated, where the CORC strand had an overall diameter

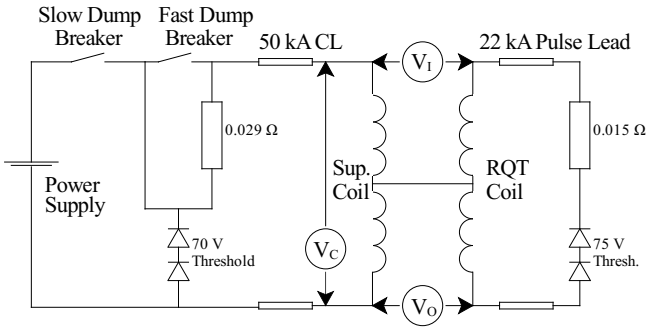

Fig. 1. Electrical scheme showing RQT protection of a superconducting magnet. Quench detection is done with three pairs of voltage taps. A slow dump (without heating in the cold mass) may be initiated by opening the slow dump breaker while a fast dump (with fast current transfer and significant heating inside the cold mass) may be initiated by opening the fast dump breaker.

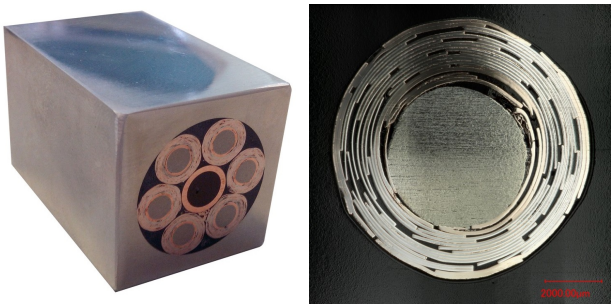

Fig. 2. Left: 6-around-1 Cable-in-Conduit (CIC) utilizing Conductor-On-Round-Core (CORC) strands. Right: Cross-section of a CORC strand, in which 38 ReBCO tapes in 12 layers, in addition to some copper tapes, are wrapped on an aluminum former. The tapes are wound clock-wise and counter-clockwise to cancel the solenoidal field component inside the strand.

of 5 mm and a critical current of 7000 A [6]. Engineering current densities in the 400-600 A/mm^2 range at 20 T are expected in the next two years [7], [8]. The production of a six-around-one cable-based 45 kA demonstration conductor is currently being finalized, in which six CORC strands are twisted around a hollow copper tube, and the cable is encased in a 30×30 mm^2 Al-5083 jacket (Fig. 2). A presentation of this geometry and measurements are found elsewhere [2], [3], [4], [5]. Recent developments in CORC-CIC technology involve a reduction in strand diameter towards 3-4 mm CORC strands [8] and utilizing solder-coated ReBCO tapes [9], for the purpose of providing a decent electrical and thermal conductance between the ReBCO layers and the CORC core, and between CORC strands. In a matter of fact by soldering the ReBCO layers in the CORC cable a solid multifilamentary ReBCO wire is born.

For the sake of the conceptual design, a conductor is envisioned with an operating current of 50 kA operating at 40 K in a background field of up to 8.5 T. A geometry is assumed in which, similarly to Fig. 2, a cable consisting of CORC strands is encased in an aluminum-alloy jacket. The strands have an outer diameter of 4 mm and the outer radius of the cable is 22 mm and about 110 CORC strands may be fitted in the cable. The strands may be twisted in an ITER-like distribution to minimize coupling loss [10]. The operating

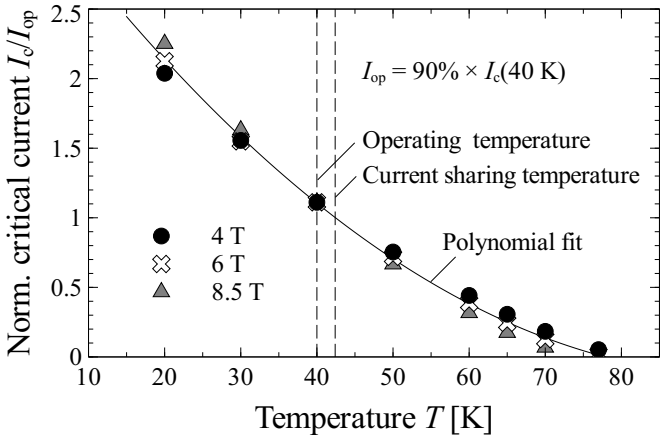

Fig. 3. Normalized critical current as a function of temperature. The temperature dependence of the normalized critical currents at 4, 6, and 8.5 T overlap and may be approximated with a polynomial fit. Data reproduced from [11].

current is at 90% of the critical current and the engineering current density of the cable is 35 A/mm^2. For comparison, the present-day record engineering current density of 340 A/mm^2 at 4.2 K and 17 T corresponds to a critical current density of well over 150 A/mm^2 at 40 K [11], which means that the required engineering current density is readily attainable.

The conductor is conduction-cooled. The absence of gas-cooling provides a simplification of conductor geometry as no voids or open spaces are needed inside the conductor and the conductor is mechanically more homogeneous. From the perspective of quench protection a direct-cooling approach is favorable as it removes heat from any potential hot-spot inside the cable, thus increasing the stability of the cable and increasing the detectability of a potential hot-spot. Thus, conduction-cooling is somewhat of a worst-case assumption.

With an oxygen-free copper core in the CORC strands, solder-coated ReBCO tapes and a minimal amount of layers, a sufficient electrical and thermal conduction between the ReBCO layers and the core is present. In addition, the CORC strands are connected by solder as well to achieve good thermal and electrical homogeneity throughout the entire cable. Achieving a good electrical and thermal exchange with the aluminum-alloy jacket (providing mechanical support to the cable) is more challenging as soldering to aluminum-alloy is not trivial. Several possibilities of achieving a sufficient thermal exchange include filling the jacket with solder or wrapping indium around the cable, by which thermal conductance is achieved through multiple pressure contacts, or impregnating the cable with a filled epoxy. The thermal bond affects the stability of the conductor and is therefore an important design feature.

B. Superconducting properties of the conductor

On the assumption of a layer-wound solenoid and considering HTS cost, grading is applied so that the operating current is at 90% of the critical current in the high-field region of each layer. The temperature dependence of the tapes with magnetic field applied in the perpendicular direction is taken

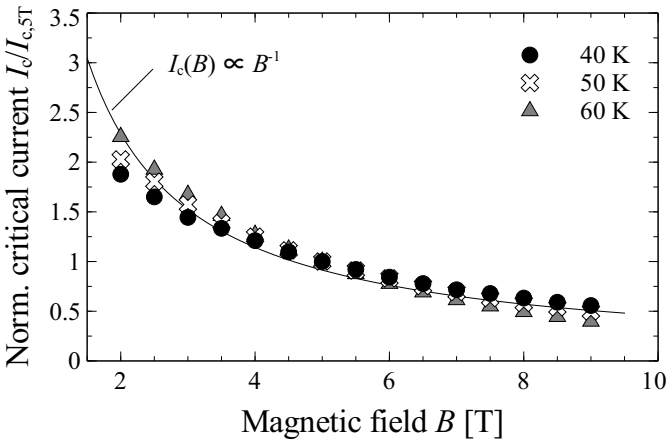

Fig. 4. Normalized critical currents as a function of magnetic field B in the 40-60 K range overlap and may be approximated as inverse to the magnetic field.

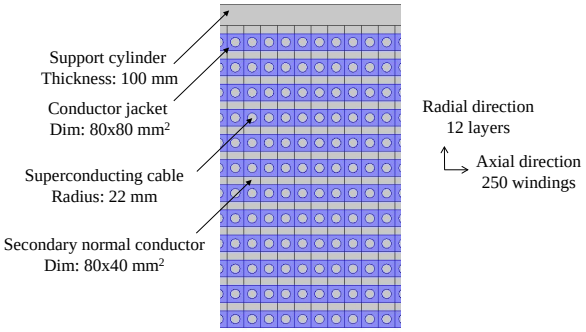

Fig. 5. Layer-wound geometry of the envisioned 50 GJ 8 T HTS solenoid operating at 40 K.

as an indication of the temperature dependence of the overall conductor. Based on data after Xu *et al.* [11], it is found that the temperature dependence of each of the layers overlaps in spite of the different local magnetic field strengths (Fig. 3). In addition, the magnetic field dependence of the critical current is found to scale approximately inversely proportional to the magnetic field in the 40 to 60 K temperature range (Fig. 4).

At a load fraction of 90% the current sharing temperature is about 2.5 K above the operating temperature of 40 K. Even though this temperature margin is comparable to the temperature margin found in the ATLAS [12] and CMS [13] conductors, the enthalpy margin is several hundred times larger resulting from the high degree of non-linearity in the heat capacity of the stabilizer. An important observation is that the critical temperature of ReBCO is significantly higher than the current sharing temperature. This means that during a quench where the local temperature does not exceed 75 K the conductor still operates in a current-sharing regime.

III. 50 GJ, 8 T, SOLENOID GEOMETRY

A simple conceptual design of a solenoid is proposed with an inner radius of 5.0 m, an outer radius of 6.4 m and a total length of 20 m. The conductor is layer-wound, with a total of 12 layers and 250 turns (Fig. 5). The superconducting layers with conductor dimensions of 80×80 mm^2 are separated by a normal layer wound from a solid Al-2.0wt%Ni alloy conductor with dimensions 80×40 mm^2.

The operating current is 49 kA; the total stored energy is 50 GJ; and the self-inductance is 41.5 H. Current ramping occurs at 70 V to allow for a complete ramp-up and ramp-down in 8 hours.

While a higher operating current is more favorable in terms of energy extraction, this would come at the cost of a bulkier conductor and an increase in bending strain. The operating current is a compromise between these two factors.

The secondary conductor comprising Al-Ni alloy performs a number of functions. Firstly, this conductor, with a yield strength of about 160 MPa as shown by Wada *et al.* [14], provides mechanical support needed for the structural integrity of the solenoid. Secondly, the combination of this geometry combined with suitable placement of the voltage taps results in a substantial reduction in the electrical noise level, thus enabling low-threshold quench detection (section V). Finally, upon quench detection this geometry allows for an immediate mitigation of the thermal runaway by fast current transfer (section VI).

Using a method described elsewhere [15] it is established that during ramping the eddy currents in the RQT conductor only amount to some watts for the entire magnet system.

IV. THERMAL SIMULATIONS

Several thermal simulations are performed, firstly to assess the minimum quench energy (MQE), i.e. the thermal energy required to induce a thermal runaway, secondly, the critical current of the conductor is locally degraded, thus illustrating a possible cause of a thermal runaway, and finally to determine how the current may be discharged while limiting the hot-spot temperature.

A. Model approximations

The electrical and thermal conductances between the ReBCO tapes, the cores of the CORC strands, and in between the CORC strands are dependent on the design of the cable and have to be investigated in detail. Here an a priori assumption is made that the electrical and thermal conductances are sufficient to ensure a homogeneous temperature within the cross-section of the cable. The thermal exchange between the cable and jacket may be non-ideal. For the sake of a qualitative investigation it is assumed that the cable is impregnated with epoxy [16], with an effective thickness of 1 mm (i.e. about a fourth of the diameter of each of the CORC strands).

The thermal conductance, electrical conductance in the normal state regime and heat capacity of the cable are dominated by high-purity copper with a residual resistivity ratio of 150 [17] which constitutes 85% of the cable. The electrical conductance to the jacket is assumed poor so that current redistribution to the jacket is neglected. The secondary conductor, comprising Al-2.0wt.%Ni, has a residual resistivity ratio of 170 [14], [18], [19]. As the magnet is operated at 40 K, the normal state resistivity of the copper and doped aluminum is already substantially higher than the residual resistivity and

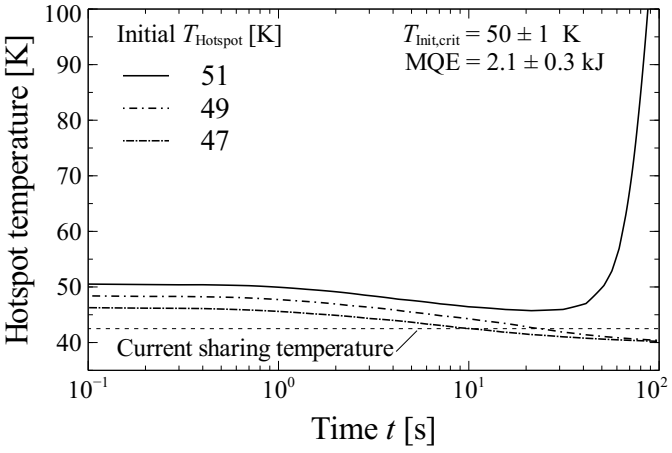

Fig. 6. Hot-spot temperature versus time after an initial temperature increase in a 200 mm hot-spot region in the superconducting conductor.

magneto-resistivity is neglected. A 1 mm thick epoxy-filled fiberglass conductor insulation is taken into account [19], while the insulation between the windings and the support cylinder is 2 mm thick.

A critical state approximation is used for the electric field over the superconducting tapes. The electric field in the current-sharing regime may be expressed as:

$$E = \rho_{\mathrm{n}}(J - J_{\mathrm{c}}(T, B)). \tag{1}$$

Here E is the electric field, ρ_{n} is the normal state resistivity, J is the current density, and $J_{\mathrm{c}}(T, B)$ is the temperature and magnetic field dependent critical current density.

Even though the proposed quench protection involves very high current ramp rates, the background magnetic field on the conductor changes very slowly with a time constant of over half an hour, thus AC losses in the conductor are neglected.

B. MQE calculation

A number of time-dependent simulations are performed under the conditions in which the local temperature in a cable section of 200 mm is raised to various temperatures above the current sharing temperature while the rest of the coil windings remains at 40 K (Fig. 6). This temperature increase results in thermal diffusion, mainly along the length of the cable, in addition to local heating. Above a certain critical initial temperature, the local heating exceeds the thermal diffusion and a thermal runaway occurs, where this critical initial temperature is dependent on the superconducting properties of the conductor and the electrical and thermal properties of the copper stabilizer. The simulations indicate a critical initial temperature of 50±1 K, which corresponds to an MQE of 2.1±0.3 kJ. This high number indicates that a thermal runaway resulting from minor conductor movement is very unlikely so that the stability of the conductor can be considered as excellent. An additional set of calculations was performed where the length of the cable section with elevated temperature was reduced to 50 mm, yielding an MQE that is identical within the error margin of the calculation.

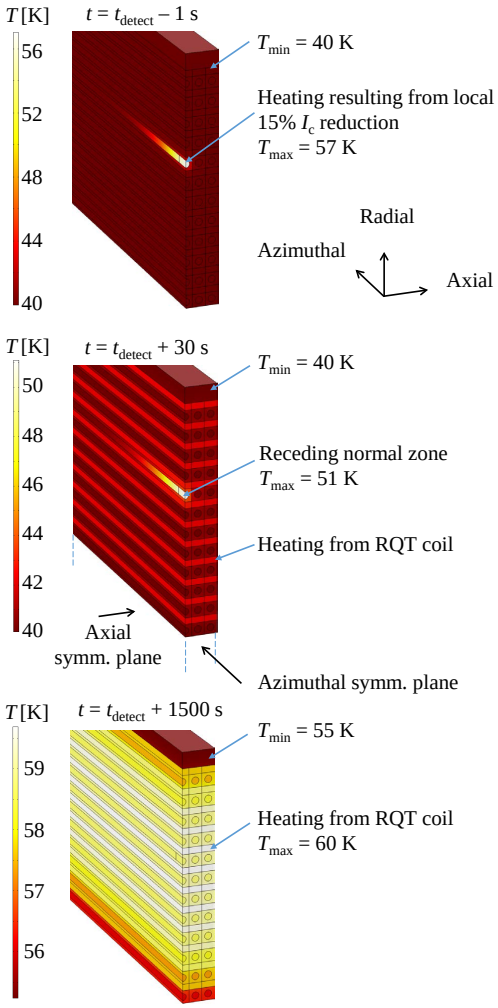

Fig. 7. Thermal evolution of a current discharge, including an initial temperature rise resulting from a 200 mm long section in the superconducting cable where critical current is degraded to 85% of nominal (top figure), a receding hot-spot region combined with an increase in overall temperature due to heating from the RQT circuit (middle figure) and long-term thermal homogeneity resulting from homogeneous heating by the RQT circuit (bottom figure). Also see Fig. 12.

C. Thermal runaway due to local critical current degradation

Even though the energy required to introduce a thermal runaway is substantial, a thermal runaway may occur if the operating current locally exceeds the critical current. Such a situation may arise due to a bad joint, a locally degraded section in the conductor, or the vicinity of an improperly cooled current lead. The impact of these possible causes is assessed in a simulation by which the critical current of a 20 mm section is reduced to 85% of the nominal critical current, which is less than the operating current (Fig. 7, top).

Due to the local heating, the local hot-spot temperature increases. As the temperature increases, the critical current density is reduced and the degree of heating increases further, so that the rate of temperature increase accelerates over time. Left unattended, the local hot-spot temperature substantially exceeds room temperature (thus implying conductor degradation) after several minutes, where the temperature rise from

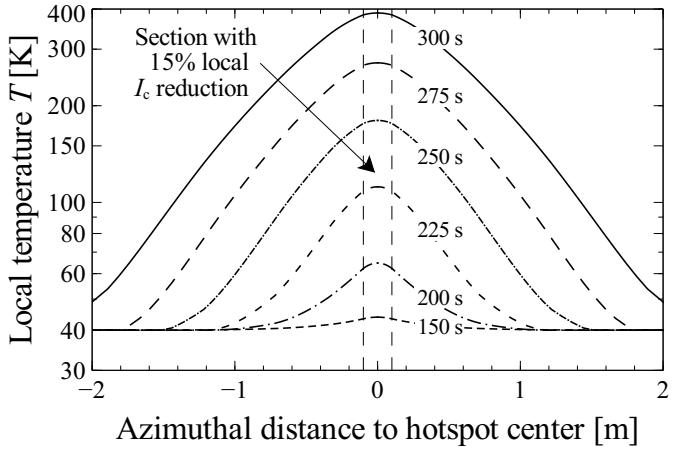

Fig. 8. Normal zone evolution during a thermal runaway resulting from local heating in a 200 mm long conductor section with a 15% reduced critical current.

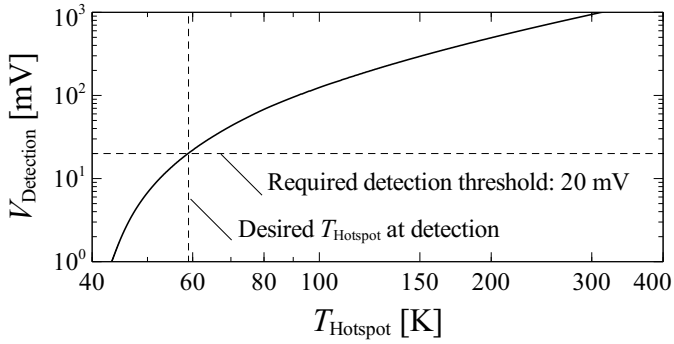

Fig. 9. Resistive voltage as a function of peak hot-spot temperature. Here, the normal zone arises during thermal runaway resulting from local heating in a 200 mm long conductor section with a 15% reduced critical current.

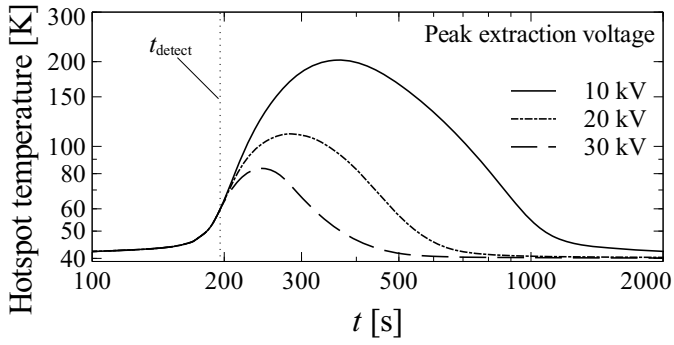

Fig. 10. Time-dependent hot-spot temperature in an alternative 'classical' protection scheme. High-voltage extraction is assumed and three potential peak extraction voltages are indicated.

60 to 100 K occurs in about 20 s. During this time, the normal zone surrounding the hot-spot slowly grows, with a characteristic velocity on the order of 20 mm/s (Fig. 8).

The resistive voltage resulting from the normal zone is shown in Fig. 9. To limit the maximum temperature difference inside the magnet to 20 K before detection, the maximum allowed voltage threshold is about 20 mV.

V. Quench Detection in Bifilar Geometry

The typical quench detection threshold in a detector magnet is on the order of 1 V [20], but the required 20 mV threshold may be achieved through the bifilar geometry of the superconducting and normal layers (Fig. 5). The magnet consists of two separate circuits, i.e. the primary circuit consisting of the superconducting layers, the current source etc., and the secondary Rapid Quench Transformation (RQT) circuit comprising the normal layers, the diodes and a second dump resistor. An electrical connection is made between the two circuits at the layer jump between the 6th and 7th superconducting layer. Voltage taps are then placed between the first layer of the primary and the RQT circuit (Voltage tap V_{I}) and the last layer of the two circuits (Voltage tap V_{O}, Fig. 1). Due to the mutual inductance between the primary and the RQT circuits, the electrical noise (emanating from the power supply) on voltage taps V_{I} and V_{O} is reduced by 99.2 and 99.8 %, respectively, in comparison to the total coil voltage (voltage tap V_{C}) before balancing. Optimal inductive balancing may be achieved with:

$$V_{\mathrm{I,balanced}} = V_{\mathrm{I}} + 0.008 \times V_{\mathrm{C}}, \tag{2}$$

$$V_{\mathrm{O,balanced}} = V_{\mathrm{O}} + 0.002 \times V_{\mathrm{C}}, \tag{3}$$

where V_{I}, V_{O}, and V_{C} are the three voltage taps on the coil (Fig. 1), and $V_{\mathrm{I,balanced}}$ and $V_{\mathrm{O,balanced}}$ are the balanced voltages on which quench detection may take place.

To get an indication of noise reduction on externally induced electro-magnetic noise, a simulation is performed in which a ramping 1 GJ solenoid is placed in close proximity to the 50 GJ solenoid. In comparison to the total coil voltage, the noise on the balanced voltage taps is 99.8 and 99.2% lower for the inner and outer balanced voltage taps respectively. Note that both voltage tap pairs are nearly independent of each other and that any resistance in the conductor leads to a positive voltage on both taps, so that the taps may be balanced against each other to further reduce electric noise. Further enhancements in noise reduction are discussed in section VII.

Recently the advantage in noise reduction of a co-wound geometry over a balanced-coil approach was experimentally demonstrated. The co-wound geometry was found to have a 80 times lower noise level [21].

VI. Rapid Current Transformation

A number of classical methods of current discharge were investigated and each of these methods was found to be problematic. The use of quench heaters for this magnet is impractical: Due to the low quench propagation velocity about 20 mm/s (Fig. 8) the entire coil needs to be heated to introduce a homogeneous quench. Moreover, the temperature has to be raised to substantially above the current sharing temperature, for instance to 60 K, in a time window of 20 s. The corresponding required power is several hundred MW, which is a highly unfeasible number. Quench-back suffers from a similar problem. The discharge voltage has to be about 1 kV while the ramping voltage is 70 V, which means that

to achieve several hundred MW of dissipation during a fast discharge, several MW needs to be cooled away continuously during ramping. A high voltage discharge is more feasible, but a peak discharge voltage above 20 kV is required to limit the hot-spot temperature to 100 K (Fig. 10).

Here, an alternative approach is used. By choosing a geometry with a very high coupling factor, current can be rapidly transferred from the superconducting coil into the RQT coil, where the current ramp speed is determined by the degree of coupling between the circuits and can therefore be orders of magnitude faster than the LR-time:

$$\frac{dI_{\mathrm{sup}}}{dt} = \left(\frac{1}{1-k^2}\right)\left(\frac{-V_{\mathrm{sup}}}{L_{\mathrm{sup}}} + \frac{MV_{\mathrm{RQT}}}{L_{\mathrm{RQT}}L_{\mathrm{RQT}}}\right), \quad (4)$$

$$\frac{dI_{\mathrm{RQT}}}{dt} = \left(\frac{1}{1-k^2}\right)\left(\frac{-V_{\mathrm{RQT}}}{L_{\mathrm{RQT}}} + \frac{MV_{\mathrm{sup}}}{L_{\mathrm{RQT}}L_{\mathrm{RQT}}}\right), \quad (5)$$

where V_{sup} and V_{RQT} are the summation of the resistive and diode voltages of the primary and RQT circuits respectively, M is the mutual induction equal to 41.9 H, L_{sup} is the self-induction of the primary coil equal to 41.5 H, L_{RQT} is the self-induction of the RQT coil equal to 42.4 H, and k is coupling factor equal to 99.91%. As previously pointed out [22], when the voltage drop over the primary circuit is significantly higher than that over the RQT circuit, the transfer time is over 500 times below the comparable LR-time. To prevent current transfer during ramp up and slow discharge, diodes are placed in series with the RQT coil so that they only conduct current when the voltage drop over the primary circuit exceeds the threshold of the diodes. Once a quench is detected, the only action that is required is to open the fast dump breaker, resulting in a very rapid transfer of just below 50% of the current into the RQT coil (Fig. 11) combined with gradual dissipation of energy over the two circuits. During the current discharge about 20% of the stored energy is homogeneously dissipated inside the RQT coil while the remainder is extracted from the system. Note that this concept is very similar to a concept previously published by Takahata *et al.* [23], except for the utilization of diodes.

During discharge, the initial voltage drop over the primary circuit is 1500 V, which drops to below 1000 V after a couple of seconds and then decreases slowly. This peak overall voltage can be reduced to about 1000 V by placing a capacitor bank with a total capacitance of 60 F parallel to the dump resistor, which also slightly reduces the speed at which current transfer occurs. This high capacitance may be achieved through the use of supercapacitors, also noting that the charge time is compatible with this type of capacitor [24].

Applying this concept to the simulation in which a thermal runaway results from a degraded section, the rapid current transfer has a strong impact on the dissipation inside the hot-spot. The hot-spot dissipation drops from about 1000 W just before quench detection to below 100 W after a couple of seconds and continues to drop until the normal zone is completely dissolved (Figs. 7 and 12). Thus, the peak temperature gradient is determined solely by the detection threshold (which may be reduced further by further optimization, section VII), and after

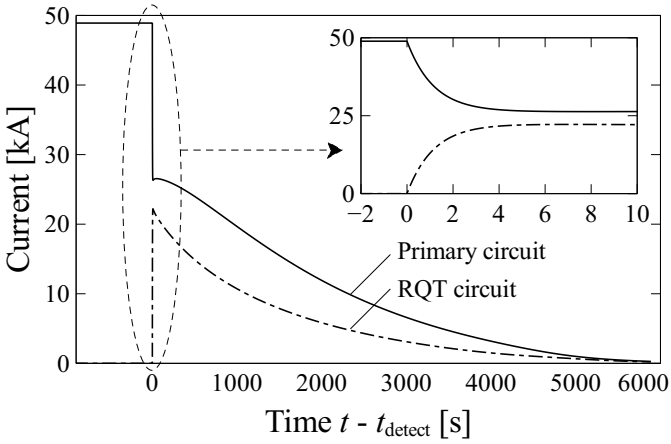

Fig. 11. Current distribution in the primary and RQT circuits before and after the quench detection. The initial very fast current transfer between circuits (see inset) is followed by a gradual energy extraction.

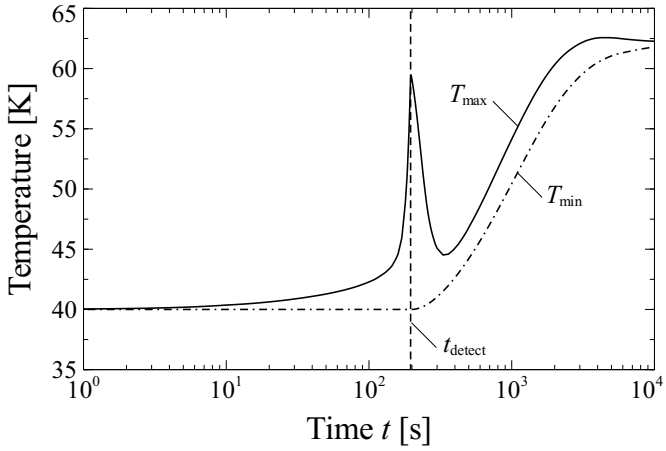

Fig. 12. Minimum and maximum temperatures inside the magnet before and after quench detection. Also see Fig. 7.

quench detection the entire coil homogeneously heats up to the final temperature of just over 60 K. With this approach nearly 80% of the stored energy is extracted. After the detection the current inside the superconductor stays below 70% of the nominal critical current until all remaining stored energy is dissipated.

VII. Further Enhancements

The concept presented here is not just suitable for very large magnets but broadly applicable for superconducting magnets that are otherwise difficult to protect. For some magnets it is desirable to not extract a large fraction of stored energy but rather dissipate the energy almost entirely into the cold mass. This can be achieved by replacing the diodes, dump resistor and fast dump breaker in the primary circuit (Fig. 1) by a superconducting switch located on the cold mass. By further increasing the degree of current transfer (but not 100% current transfer, to avoid local tensile stress in coils without pre-compression) either by raising the maximum allowed voltage drop over the superconducting switch, reducing the resistivity of the RQT conductor or changing the geometry nearly all the

stored energy may be homogeneously dissipated in the RQT circuit. In addition, this concept may be applied to a string of superconducting magnets by placing a bypass diode parallel to the superconducting coil and superconducting switch, enabling each magnet to discharge individually.

The concept presented here may be optimized further by using multiple RQT circuits rather than a single circuit, where each circuit has an electrical connection to the primary circuit and two pairs of voltage taps. This features a number of benefits. Firstly, with more voltage taps monitoring smaller conductor sections the noise level per voltage tap pair is further reduced. Secondly, the system has more degrees of freedom so that current transfer occurs even faster. Thirdly, the peak layer-to-layer voltage is given by the length of the RQT conductor, and in the scheme shown in Fig. 1 is equal to half the peak discharge voltage. By subdividing the RQT circuit, this peak layer-to-layer voltage may be reduced. Note that the current distribution between the RQT circuits is subject to a negative feedback loop and is therefore stable: if one of the circuits is warmer than the other ones, the resistance of this circuit is higher and current is transferred out of this circuit, and the other RQT circuits can catch up in temperature.

VIII. Discussion

A number of worst-case assumptions were used for the thermal simulations. For instance, it is not unreasonable to expect a future conductor design with non-negligible electrical and improved thermal exchange between cable and jacket, which would further enhance the stability of the conductor. This serves to illustrate one of the main conclusions of this paper: even under pessimistic assumptions, the protection of a large HTS magnet operating at 40 K is challenging but feasible. Moreover, from the perspective of stability and quench protection a good thermal and electrical conductance between cable and jacket is preferable but not strictly mandatory.

It is not proven that the superconductor assembly behaves as a thermally and electrically homogeneous conductor and indeed the validity of this assumption is dependent on the design of the conductor. A dedicated model for analyzing the local electrical and thermal responses of a quenching conductor is required to make this assessment, which is beyond the scope of this paper. For the moment, if the amount of tapes per CORC strand is minimized and the CORC strands are properly soldered together then the assumption of good thermal and electrical conductance inside the superconducting cable seems reasonable.

The feasibility of obtaining the various electrical components was not investigated in depth. For instance, this design requires diodes that can sustain up to 50 kA over an extended period of time for the slow extraction of stored energy. Note however, that arrays of 20 kA diodes are used in the ATLAS magnets [25], which suggests that systems of 50 kA diodes can be qualified as well. Moreover, as in the design by Takahata *et al.* [23], the diodes may be replaced by breakers and resistors at the cost of increasing the number of actions required for energy extraction.

As a general observation, the approach used in this paper works by substantially increasing the MQE so that the superconducting cable recovers. If for whatever reason a sufficiently high hot-spot temperature is reached before current transfer occurs, the current remaining in the primary circuit will still be sufficient to cause a thermal runaway, albeit at a significantly reduced rate. This issue may be improved by further increasing the degree of current transfer (which may for instance come at the cost of a higher peak voltage, or an increase in the RQT conductor size or both). To illustrate, in the fully normal regime a 50% current transfer results in a four-fold reduction in dissipation inside the superconducting cable versus the scenario without current transfer, and 75% current transfer results in a sixteen-fold reduction.

Note that while the RQT concept was used to achieve quench recovery in this conceptual design, another approach that could have been taken is to induce a normal zone throughout the coil winding by dissipating more heat in the RQT circuit. The latter approach is particularly applicable and likely unavoidable for low temperature superconductors where bringing the superconducting conductor into normal state requires a relatively small amount of energy. For HTS-type superconductors the choice between the two options is essentially a design choice, where the choice for the first option was taken here to achieve a greater level of extraction.

IX. Conclusion

A series of calculations were performed to provide insight in the quench behavior of a very large 50 GJ 8 T HTS-based magnet operating at 40 K and utilizing CORC-CIC technology. It is found that while the ReBCO-based CORC-CIC cable is expected to be extremely stable with a minimum quench energy in the kJ range, the quench propagation velocity is very low and the time window in which thermal runaway occurs is very short in comparison to the attainable extraction time for a low-voltage system. This means that classical quench protection solutions such as heaters and quench back are not feasible and that, utilizing the classical extraction solution, high-voltage extraction would be required to maintain an acceptable hot-spot temperature. A novel 'Rapid Quench Transformation' concept, which involves rapidly transferring a large fraction of the current into a secondary normal circuit, is proposed and presented. Due to a co-wound geometry this concept helps to substantially lower the electrical noise on the quench detection voltage taps as well and low-threshold quench detection is applied. After quench detection fast current transfer is initiated by opening a single breaker. The concept works in coil ramping conditions (with no transfer during regular ramping), does not require an external energy source, may be used to either extract most energy or homogeneously dissipate the stored energy inside the magnet and is compatible with bypass diodes for use in a string of magnet systems. Applying this concept to the 50 GJ magnet system, the electrical and thermal simulations indicate that once a thermal runaway occurs, nearly 80% of the energy is extracted, the hot-spot temperature is kept with 20 K of the cold mass temperature, and the overall temperature is kept well below 100 K without requiring a large extraction voltage.

REFERENCES

[1] D. .C. van der Laan, "$YBa_2Cu_3O_{7-\delta}$ Coated Conductor Cabling for low AC-loss and High-field Magnet Applications", Supercond. Sci. and Technol. 22, 065013 (2009).

[2] T. Mulder, A. Dudarev, M. Mentink, M. Dhalle, and H. ten Kate, "Development of joints for a new six-around-one CORC based ReBCO Cable-inConduit Conductor rate 45 kA at 10T/4K", To be published in IEEE Trans. on Appl. Supercond., (2015).

[3] T. Mulder, A. Dudarev, D. van der Laan, M. Mentink, M. Dhalle, and H. ten Kate, "Optimized and practical electrical joints for CORC type HTS cables", To be published in IOP Conf. Ser. Mat. Sci. and Eng., (2015).

[4] T. Mulder, A. Dudarev, M. Mentink, D. C. van der Laan, H. Silva, M. Dhalle, and H. ten Kate, "The first 45 kA at 10 T CORC based ReBCO Cable-in-Conduit for large scale magnets", To be published in IEEE Trans. Appl. Supercond., (2015).

[5] T. Mulder, A. Dudarev, M. Mentink, D. C. van der Laan, M. Dhalle, and H. ten Kate, "ReBCO-CORC hairpin characterization for high field applications", To be published in IEEE Trans. Appl. Supercond., (2015).

[6] D. van der Laan, M. Mentink, A. Dudarev, T. Mulder, and H. ten Kate, "Towards 3 mm diameter CORC cables utilizing ReBCO technology", Presented at the Magnet Technology conference, Seoul (2015).

[7] D. van der Laan, L. Bromberg, P. Michael, J. Minervini, T. Mulder, and H. ten Kate, "Development of HTS Conductor on Round Core (CORC) Cables for Fusion Application", Presented at the HTS4Fusion workshop, Pieve Santo Stefano (2015).

[8] Cryogenic Society of America, Inc., "Development of HTS CORC Cables for High Field Magnets and Advanced Power Transmission", www.cryogenicsociety.org.

[9] K. Yagotintsev, K. J. Huang, M Dhalle, P. Gao, T. J. Haugan, D. C. van der Laan, R. Wesche, D. Uglietti, W. Goldacker, A. Kario, L. Muzzi, A. Della Corte, and A. Nijhuis, "AC Loss in REBCO Cables, Influence of Inter-tape Resistance and Twist Pitch", Presented at the HTS4Fusion workshop, Pieve Santo Stefano (2015).

[10] E. P. A. van Lanen, J. van Nugteren, and A. Nijhuis, "Full-scale calculation of the coupling losses in ITER-size cable-in-conduit conductors", Supercond. Sci. Technol. 25, 025012 (2012).

[11] A. Xu, V. Braccini, J. Jaroszynski, Y. Xin, and D. C. Larbalestier, "Role of weak uncorrelated pinning introduced by $BaZrO_3$ nanorods at low-temperature in (Y,Gd)$Ba_2Cu_3O_x$ thin films", Phys. Rev. B. 86, 115416 (2012).

[12] ATLAS Magnet Project Collaboration, "ATLAS Barrel Toroid", Technical Design Report (1997).

[13] CMS Collaboration, "CMS, the Magnet Project", Technical Design Report (1997).

[14] K. Wada, S. Meguro, H. Sakamoto, A. Yamamoto, and Y. Makida, "High-strength and High-RRR Al-Ni Alloy for Aluminum-Stabilized Superconductor", IEEE Trans. on Appl. Supercond. 10, p. 1012 (2000).

[15] G. Moritz, "Eddy Currents in Accelerator Magnets", presented at CAS Magnets, Bruges (2009).

[16] Y. J. Chen, X. J. Ren, P. Zhang, T. Zhang, and A. B. Wu, "Measurement of Thermal Conductivity of CFRPs and Thermal Conductance of the Cold-to-Warm Joint at Low Temperatures", IEEE Trans. on Appl. Supercond. 22, p 7700704 (2012).

[17] NIST Cryogenic Technologies Group, "Material Properties: OFHC Copper (UNS C10100/C10200)", www.cryogenics.nist.gov.

[18] P. D. Desai, H. M. James, and C. Y. Ho, "Electrical Resistivity of Aluminum and Manganese" J. Phys. Chem. Ref. Data 13, 1131 (1984).

[19] E. D. Marquardt, J. P. Le, and R. Radebaugh, "Cryogenic Materials Properties Database", presented at the 11th Int. Cryoc. Conf., Keystone (2000).

[20] P. Fazilleau, D. Campi, B. Cure, A. Herve, F. Kircher, C. Lesmond, and G. Maire, "Analaysis and Design of the CMS Magnet Quench Protection", IEEE Trans. on Appl. Supercond. 16, 1753 (2006).

[21] T. Ariyama, T. Takagi, D. Nakayama, E. Sasaki, T.Takao, O. Tsukamoto, and T. Matsuoka, "Quench Detection Characteristics of Co-winding Method and Conditions for Quench Protection of YBCO Coils", Presented at the EUCAS conference, Lyon (2015).

[22] P. F. Smith, "Protection of Superconducting Coils", Rev. Sci. Instrum. 34, 368 (1963).

[23] K. Takahata, T. Mito, H. Tamura, S. Imagawa, and A. Sagara, "Internal Energy Dump for Superconducting Magnet Protection of the LHD-type Fusion Reactor FFHR", Presented at the Int. Stellerator / Heliotron worksh, Toki (2007).

[24] Battery University, "How Does a Supercapacitor Work", www.batteryuniversity.com.

[25] A. Dudarev, A. Gavrilin, H. ten Kate, D. Baynham, M. J. D. Courthold, and C. Lesmond, "Quench Propagation and Protection Analysis of the ATLAS Toroids", IEEE Trans. on Appl. Supercond. 10, 365 (2000).